Sam Baugh
Time Dependent Statistics
Final Project

1 Abstract

In this report, we use a variety of time series techniques to analyze the "Seasonal Central England Temperature, 1659 to 2016" dataset. In section 2, we use visulization techniques to gain intuition about the dataset. In section 3, we use time domain techniques to model the variance of the series. We th en proceed to fit frequency domain models to the de-trended dataset in section 4. In section 5, we use predictive versions of our previous models in order to evaluate the warming trend in the dataset seen after year 1900. We then address the warming trend of the series. Finally, we use variations on our findings to evaluate claims made in papers/articles written by Jones and Bradley (1992a), Benner (1999) and Vaidyanathan (2016).

2 Visualizing the Data

Many of the most effective models for analyzing data rely on external assumptions. For example, many climate scientists analyze temperature data using models based off of theories of climate science, for example Brenner's analysis of sunspot cycles (Brenner 1999). In this project, we wish to analyze the data without knowledge of these external factors. As such, all of our models must be based on trends observed in the data alone. We will first attempt to develop theories regarding trends in the dataset using visualizing techniques prior to testing these trends formally. Naturally, there is a certain level of imprecision in this method, which is why models that are based off of actual scientific theories are preferred. However there is an advantage in that this 'naive' method is free from making errors related to the imprecision in scientific theories (that is, we cannot really precisely quantify the effect of sunspots on central England temperature data). We begin with a simple plot of the temperature data against time in Figure 1.

Figure 1 does not tell us very much about the data, however we can see that the mean does not appear to be constant (as it looks like it increases over time) and as such we do not suspect that the series is stationary. It also looks like there might be some periodic correlations, but nothing that we can observe directly. We suspect

Figure 1: Time series of yearly averaged data.

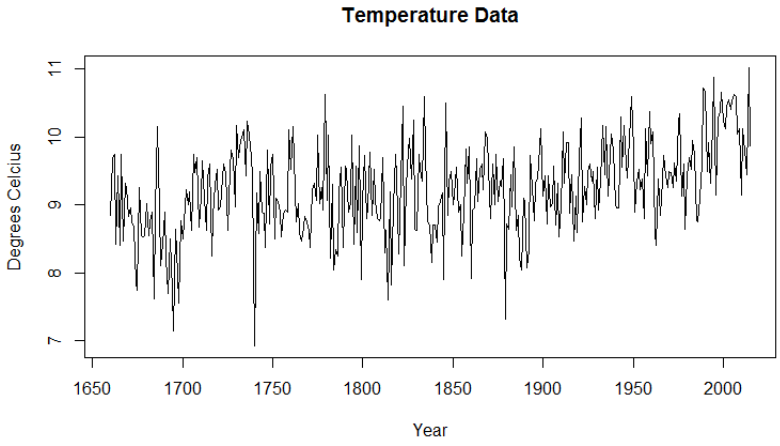

that there is a trend in the mean of the data, which we would want to avoid in order to achieve stationarity. We get similar information from seasonal data (see Figure 2).

Figure 2: Time series of seasonal data.

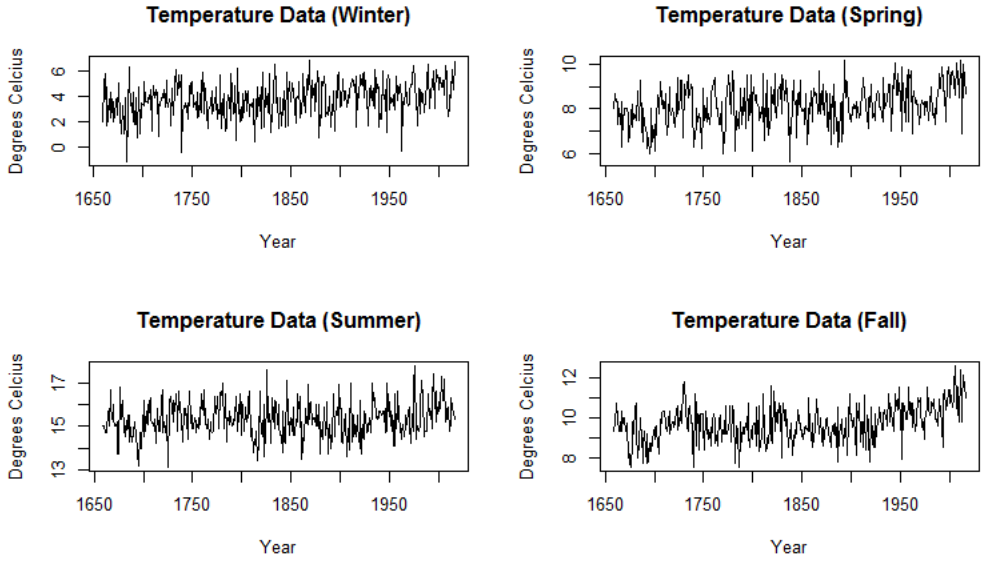

Note that in the seasonal graphs, we denote 'Winter' as December, January, and February, 'Spring' as March, April, and May, 'Summer' as June, July, and August, and 'Fall' as September, October, and November. From Figure 1 and Figure 2 graphs alone we can't entirely assess the autocorrelations, and as such we plot the acfs in Figure 3 and Figure 4. In Figure 3, we see strong auto-correlations throughout the

Figure 3: Autocorrelation of yearly averaged data.

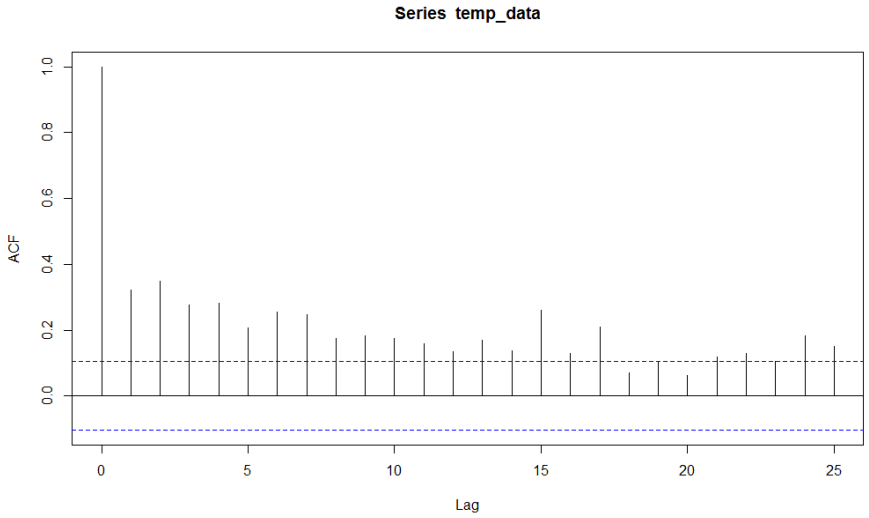

Figure 4: Autocorrelation of seasonal data.

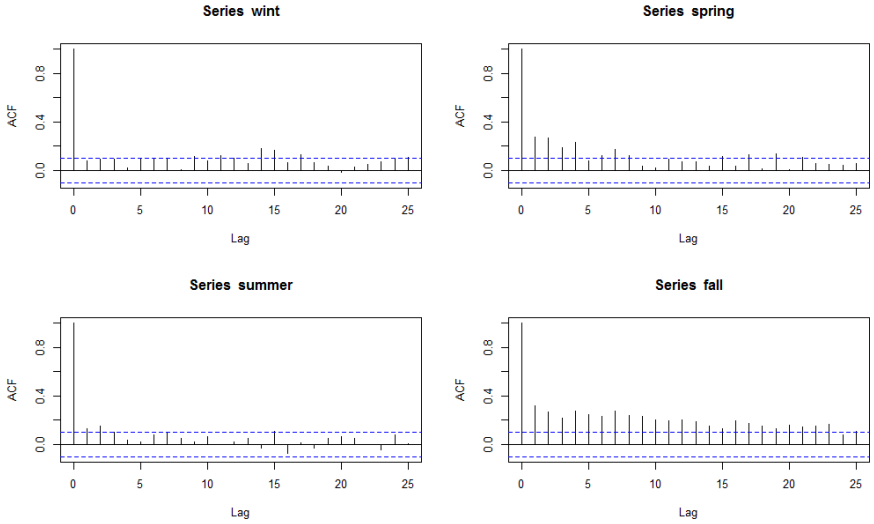

yearly data that are most likely an indicator of *non-stationarity* in the variance. We see the same in Figure 4 for the most part, however we also see significant seasonal difference (winter has very little correlation, while fall has a large amount of correlation). Overall, we conclude that yearly averaged data *non-stationary*, that there is probably a an increasing trend, and that there are seasonal differences in the autocovariance.

We suspect that we could determine the trend of the data by abstracting some of

the significant noise present. Filters and kerneling techniques are designed for this purpose. To begin, we apply a moving average filter to the data (which we set at $lag = 25$, as setting the lag lower does not sufficiently abstract the noise). See Figure 5.

Figure 5: Smoothed yearly data.

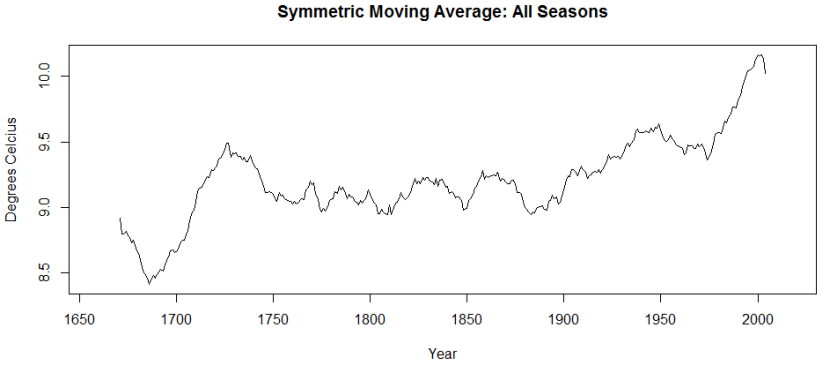

This breaks down into the following seasonal moving average plots, with the same filter, in Figure 6.

Figure 6: Smoothed seasonal data.

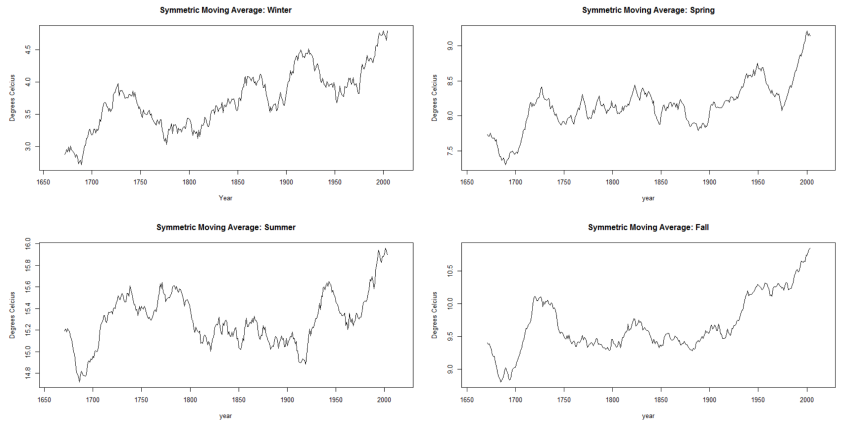

Given the moving-average-smoothed yearly data in Figure 5, we make the following observations: the data seems to start with a downward trend, acquire an upward trend throughout the 1700s, level out over the next two hundred years, and then acquires an upward trend beginning in the early 1900s that markedly accelerates towards the end of the 20th century. This raises the following suspicions: the trend may

be modeled as perhaps a cubic or quartic polynomial (there are multiple inflection points), there is reason to think that there is 'global warming' after the 1950s, and natural periodic behavior found in the late 1700s through early 1900s section may be obscured by less consistently periodic behavior at the beginning and end of the data set. We will formally investigate these suspicions in *section 5*. We also note that this plot agrees with our suspicion that the mean of the series is not constant.

Figure 6 is very interesting, as it shows the same *general* trends as the yearly averaged data in Figure 5, however each season shows fairly different periodic behavior. We suspect that the detrended series will exhibit different periodic behaviors; we will formally investigate this suspicion in *section 4*.

The main benefit of these moving average filter visualizations is that we are able to see large, long-term trends. However, much information is lost through the strength of the filter. In order to compensate we will also use *kernel smoothing* and *lowess smoothing*. In Figure 7 we use the normal kernel (we choose a bandwidth of 5 after experimenting with several different bandwidths):

Figure 7: Kernel Smoother with Bandwidth 5

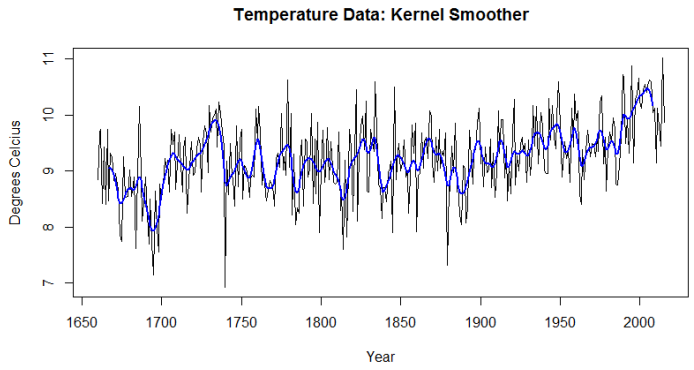

Figure 7 shows possible periodic components more strongly than the moving average filter. However, it is less useful for observing the general trends (in Figure 7, the increase in warming in the 1600s and 1900s is very subdued). In order to show the long-term trends better, we fit the lowess smoother with parameter 1/10 (also determined through experimentation), generating Figure 8.

Figure 8 is fairly smooth, but we can nevertheless identify the main trend (this graph supports our previous suspicion that a cubic or quartic polynomial is the best indicator

Figure 8: Lowess Smoother with Bandwidth 1/10

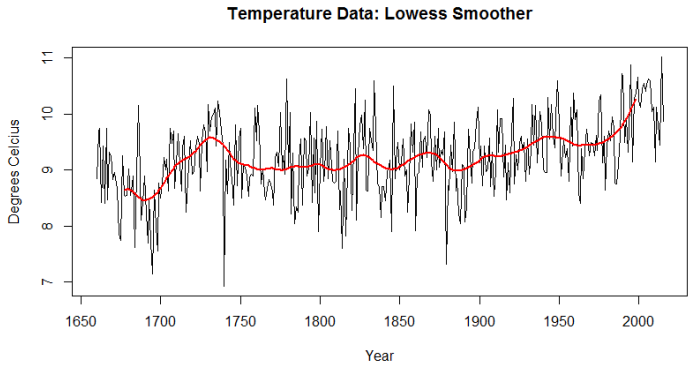

of trend). Additionally, we can see that the periodic behavior at the ends of the data set is more subdued (an observation supported by the moving average filter, but not really seen in the kernel smoother). Note that we do not fit kernel or lowess smoothers to the individual seasons, because the relationship between them in the moving average filter is very similar to the relationship between the lowess/kernel smoother for the yearly data with the moving average filter for the yearly data.

3 Time Domain Models

After visualizing the data in the previous section, we suspect that the data contains periodic components as well as a strong trend. We know that these periodic components can be represented through an ARMA process, but because the data appears non-stationary we must first apply a transformation first. First we will show that a linearly de-trended model is insufficient. Then we experiment with differencing and higher order polynomial de-trending.

```
lm(formula = rowMeans(mydata) ~ years[-1][-357])

Coefficients:
Estimate Std. Error t value Pr(>|t|)
(Intercept)     4.3378198  0.5954251   7.285 2.10e-12 ***
years[-1][-357] 0.0026616  0.0003235   8.227 3.72e-15 ***

Adjusted R-squared:  0.1581,  p-value: 3.718e-15
```

This coefficients of this model are very significant, as expected. In order to visualize

whether or not this is a good model, we will first plot the de-trended series in Figure 9.

Figure 9:

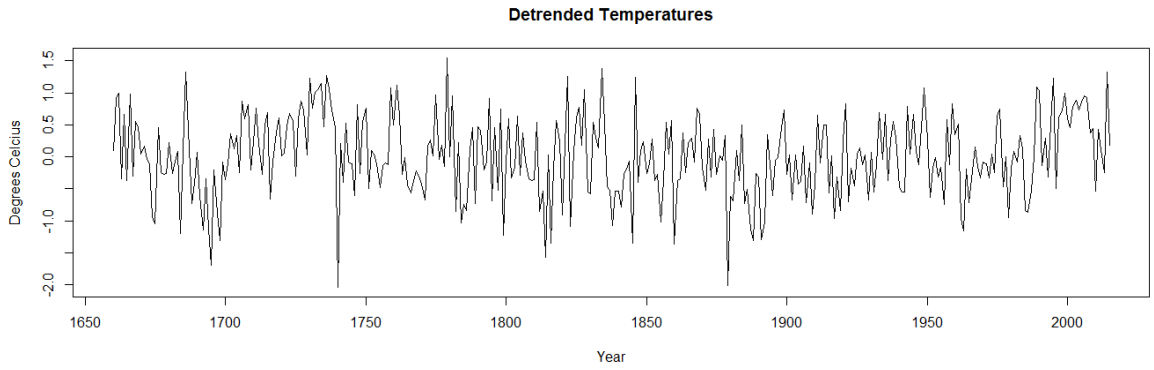

Figure 9 does not appear completely stationary, as the mean does not quite seem constant and there seems to still be some strong autocorrelations. We want to compare the linearly detrended series with the differenced series to see if it is appropriate to fit an ARIMA model, and as such we plot the first differenced series in Figure 10.

Figure 10:

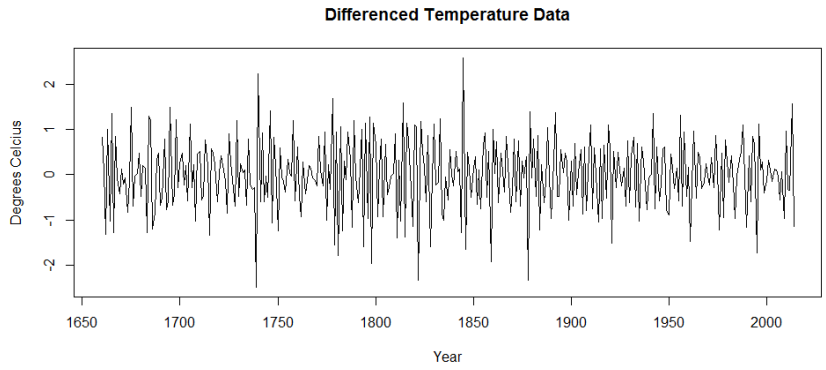

This appears to be more stationary, as there does not appear to be any reugular periodic components and the mean seems to be constant. We verify these assumptions by looking at the acf plots for each series and comparing (see Figure 11), where the differenced data acf looks the most stationary.

We conclude that the first differenced series is superior than the linearly de-trended model, because the shape of the acf for the first differenced process appears to be

Figure 11:

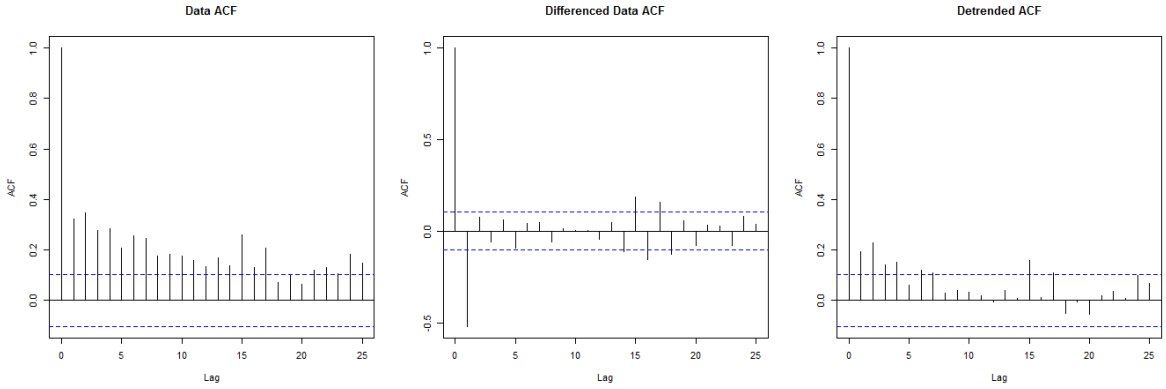

that of am MA(2) process. On the other hand, the linearly de-trended series shows the same patterns as the non-stationary original process. Now we will compare the first differenced series with further differencing (see Figure 12)

Figure 12:

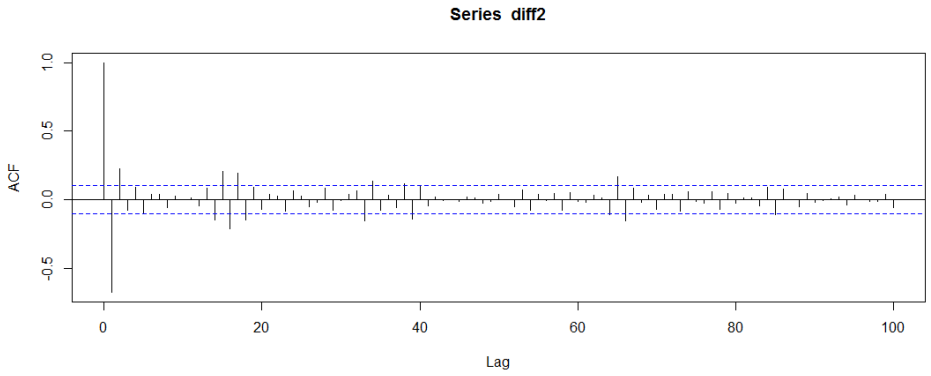

Figure 12 shows no evidence that the first differenced series is in any way more suitable than the second differenced series, so we stick to the first differenced series as we do not want to overdifference (doing so could yield unnecessary dependence). We stated earlier that the first differenced series appears to be stationary and looks characteristic of an MA(2) process. From the time plot (Figure 13), it appears that the mean and variance are constant with respect to time, so we can test for a unit root (for stationarity) using the df, adf, and pp tests. As such we run the following R-code (where diff1 is the first differenced series):

```
adf.test(diff1, k=0) # DF test
```

```
adf.test(diff1) # ADF test
pp.test(diff1)
```

We get a Dickey-Fuller value of -32.127 and a p-value of less than 0.01, a Dickey-Fuller value of -9.4246 and a p-value of less than 0.01, and a Dickey-Fuller value of -449.89 with a p-value of less than 0.01 (respectively), all against a null hypothesis of explosive and an alternative hypothesis of stationary. Thus, we reject the null hypothesis and conclude that the first differenced series is stationary.

Figure 13:

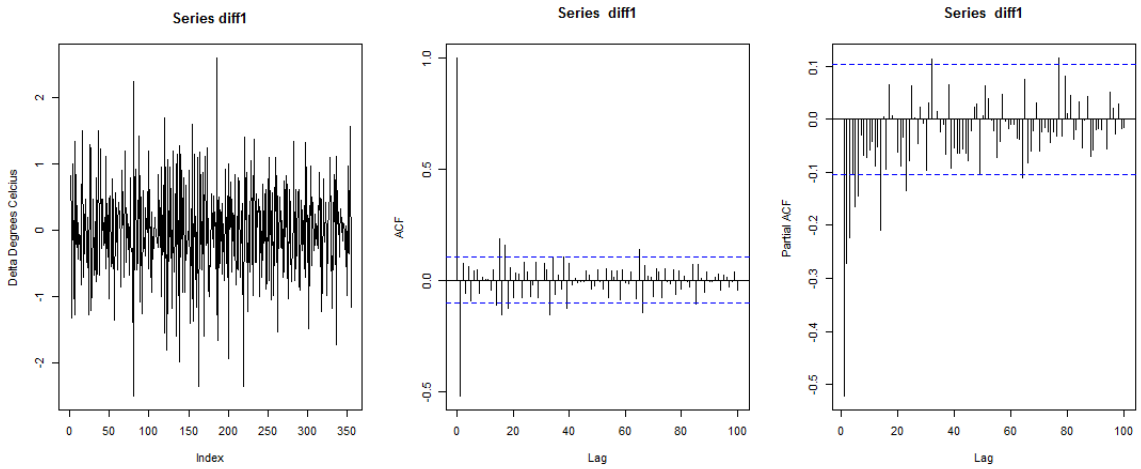

Because the process is stationary and the acf and pacf in Figure 13 is characteristic of an MA(2) process (as outlined by Table 3.1 in the textbook), it is appropriate to fit an ARIMA$(p, 1, q)$ model where $p = 0$, $d = 1$, and $q = 2$. This is exactly accomplished by the following R-code with results and diagnostic plot (Figure 14):

```
sarima(temp_data,0,1,2)
Coefficients:
ma1      ma2  constant
-0.8444  -0.0436    0.0033
s.e.   0.0490   0.0531    0.0037
```

The diagnostic plots in Figure 14 shows that this model is appropriate: inspection of the time plot of the standardized residuals shows no obvious patterns. There are some outliers in the residual plot, however, that exceed 3 standard deviations in magnitude. The ACF of the standardized residuals show no apparent departure from the model assumption (there a couple of significant autocorrelations, but none are particularly

Figure 14: Diagnostic Plots for ARIMA$(0, 1, 2)$ (generated by 'sarima' in R)

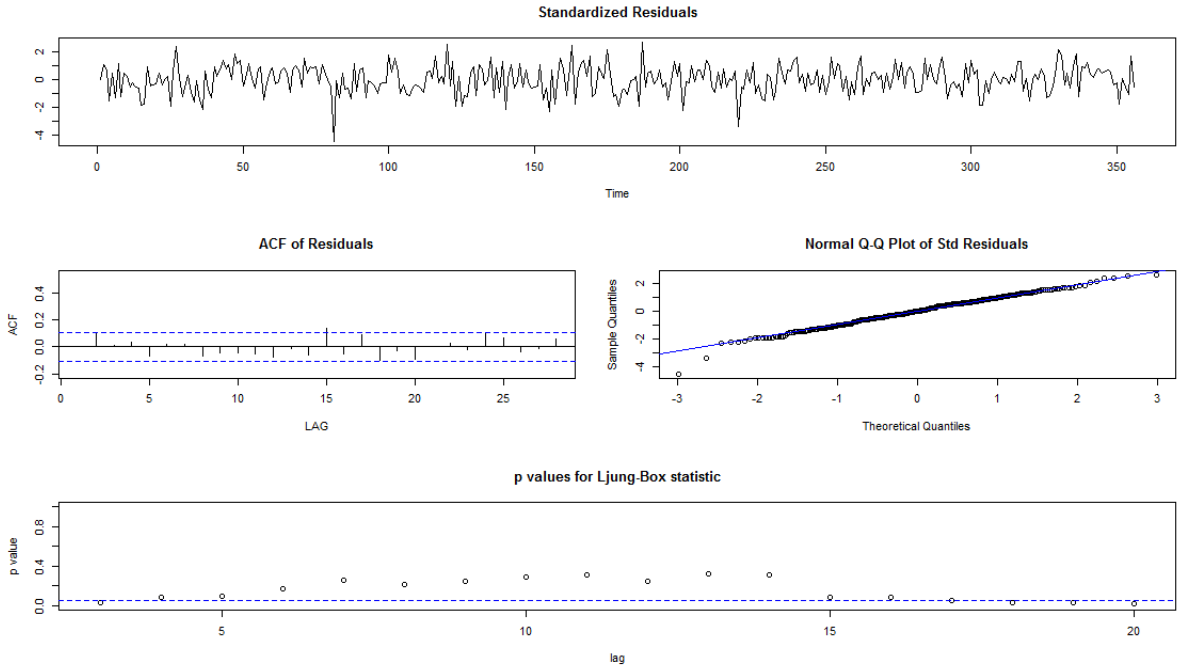

large or consistent). The QQ plot shows some departure from normality at the tails, which is undesirable but acceptable. Some of the p-values for the Ljung-Box statistic (the test for the stationarity of the model) are below the $\alpha = 0.05$ significant level for some lags (giving evidence that the model isn't stationary at these lag values) however they do not appear to be significant at $\alpha = 0.01$. While this model is acceptable, the large number of $\alpha = 0.05$ significant Ljung-Box p-values for higher lags gives us suspicion that the data might be long-memory and as such be over differenced with a fully integrated $d = 1$ ARIMA model. As such, we will attempt to fit a fractional differenced (or long-memory) model. To do so, we run the following code in R:

```
logtemp = log(temp_data)-mean(log(temp_data))
temp.fd = fracdiff(logtemp, nar=0, nma=2)
temp.fd$d
temp.fd$stderror.dpq
p = rep(1,31)
for (k in 1:30){ p[k+1] = (k-temp.fd$d)*p[k]/(k+1) }
plot(1:30, p[-1], ylab=expression(pi(d)), xlab="Index", type="h")
res.fd = diffseries(log(temp_data), temp.fd$d)
res.arima = resid(arima(log(temp_data), order=c(1,1,1)))
```

```
par(mfrow=c(2,1))
acf(res.arima, 100, xlim=c(4,97), ylim=c(-.2,.2), main="")
acf(res.fd, 100, xlim=c(4,97), ylim=c(-.2,.2), main="")
```

Figure 15: Fractional Differencing Diagnostics

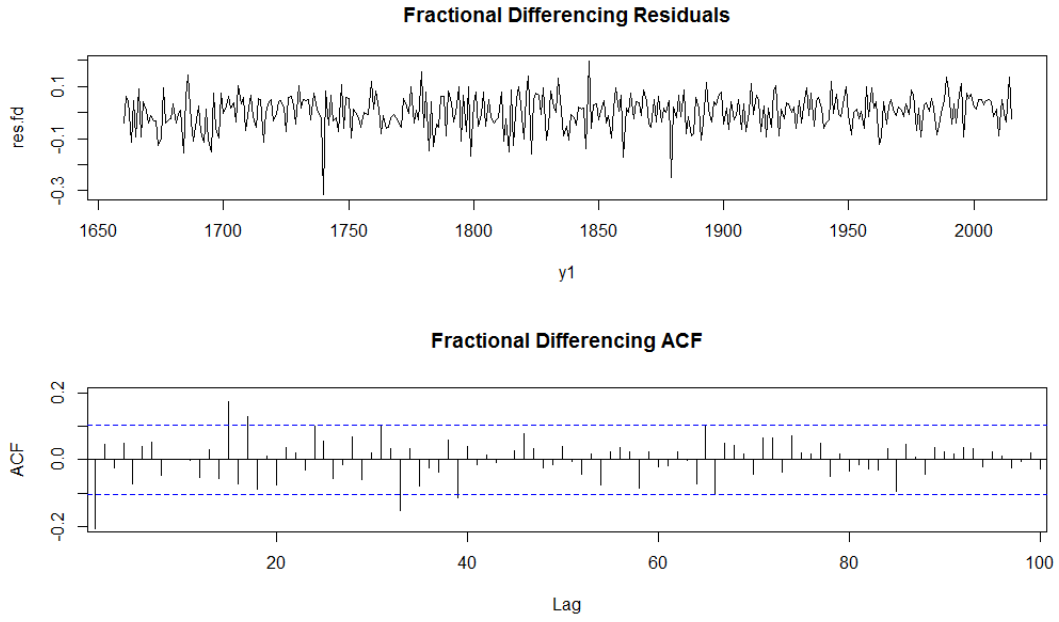

We get the fractional differencing with moving average degree two (the model ARFM$(0, \hat{\delta}, 2)$) parameters of $\hat{d} = 0.3592807$, $\hat{\theta}_1 = 0.20921095$, $\hat{\theta}_2 = -0.04589508$. The corresponding standard errors are as such: $se_{\theta_1} = 0.039542423$, $se_{\theta_2} = 0.043260411$, and $se_d = 0.005512709$. We present the diagnostics in Figure 15. In Figure 15, we see that the residuals plot is reasonable (with some notable outliers), as well as the acf plot (even though some correlations are strongly correlated). However, these plots do not convince us that a fractional differencing model is significantly preferable to the fully integrated model, ARIMA$(0, 1, 2)$, as previously discussed.

4 Frequency Domain Models

In *section 3*, we apply time domain models to model the data. We know from the spectral representation theorem for stationary processes (Theorem 4.1 in the book) that any stationary process can be represented as the random superposition of sines

and cosines oscillating at various frequencies. As such, we need to make this series stationary in order to analyze the periodic behavior from a frequency domain approach. In *section 3*, we discovered that the first differenced process is stationary. However, the periodogram of the first differenced series is not very insightful, as can be seen in Figure 16.

Figure 16: Differenced Periodogram

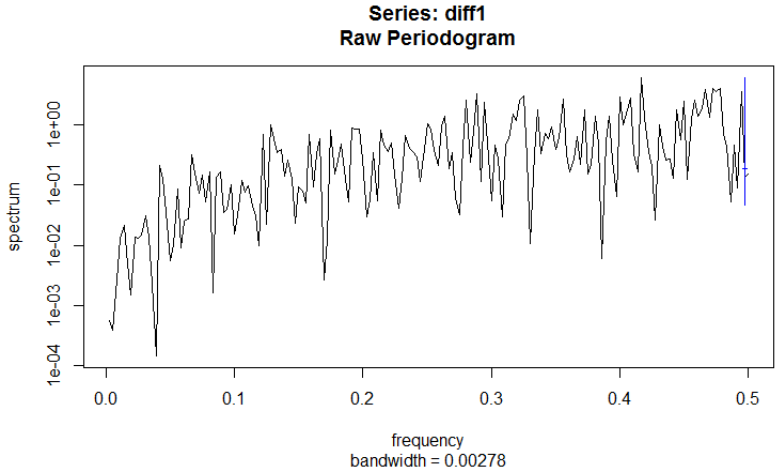

We determined in *section 3* that the linear trend model is insufficient for creating a stationary de-trended process. As such, we are going to try to identify a trend using a higher order polynomial. Recall *section 2*, where we speculated from the moving average smoothed series that the trend could be possibly modeled by a cubic or quartic polynomial. The linear model fitted to the yearly temperature data had significant coefficients, as well as fitted quadratic model (not shown). As such, we will see if a cubic model has significant coefficients. When we run the regression of the temperature data on a cubic model using R code, we get the following output:

```
Coefficients:
Estimate Std. Error t value Pr(>|t|)
(Intercept) -8.432e+02  2.338e+02  -3.606 0.000355 ***
y            1.411e+00  3.829e-01   3.685 0.000265 ***
I(y^2)      -7.784e-04  2.087e-04  -3.729 0.000224 ***
I(y^3)       1.431e-07  3.786e-08   3.780 0.000184 ***
```

The coefficients are all significant at the $\alpha = 0.001$ level. As such, we conclude that this is an appropriate model for the trend of the year-averaged temperature data. It

should be noted that we identified four components to the moving averaged smoothed series as plotted in *section 1*, which gave us reasoning to suspect suspect that the trend could be modeled with a quartic polynomial instead of a cubic. In order to evaluate this suspicion, we ran the regression of the temperature data on a quarter model in R, with the output displayed below. As none of the coefficients are significant, we conclude that a cubic polynomial is the best polynomial model of the trend. We plot the trend in blue over the dataset in Figure 17, and as we can see it appears to be a reasonable assessment of the trend.

```
Coefficients:
Estimate Std. Error t value Pr(>|t|)
(Intercept) -4.018e+02  4.785e+03  -0.084    0.933
y            4.461e-01  1.045e+01   0.043    0.966
I(y^2)       1.135e-05  8.553e-03   0.001    0.999
I(y^3)      -1.438e-07  3.107e-06  -0.046    0.963
I(y^4)       3.903e-11  4.226e-10   0.092    0.926
```

Figure 17: Temperature Data with Trend

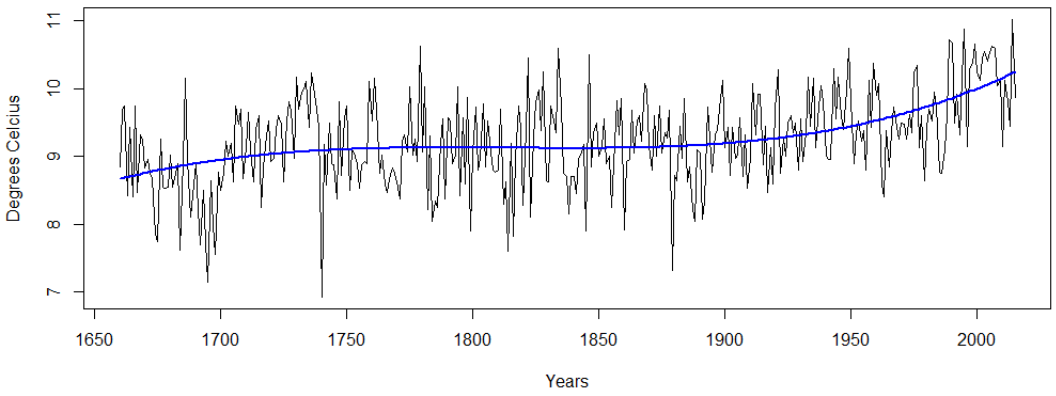

In Figure 18, we see the series de-trended with respect to the cubic polynomial previously fitted. This appears to be stationary, as the mean and variance seem constant with respect to time. This impression is confirmed by the unit root test. This is further evidenced by examining the acf plot in Figure 19, which shows structured autocorrelations similar to that of the differenced series analyzed shown in the previous section. We would like to note that this acf is much more well-behaved than the acf of

Figure 18: Detrended Temperature Data, Overall

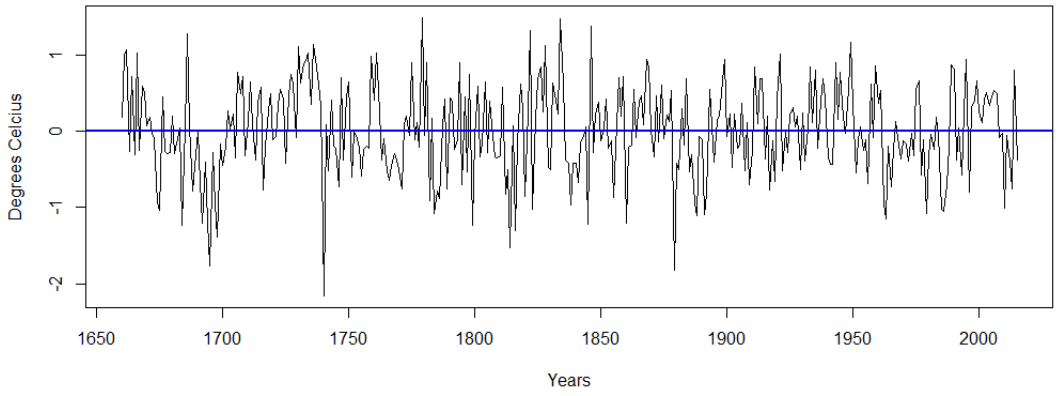

the linearly de-trended series investigated in the previous section, further indicating the suitability of the cubic polynomial in modeling the trend. As this de-trended series is stationary, we plot the periodogram in Figure 20.

Figure 19:

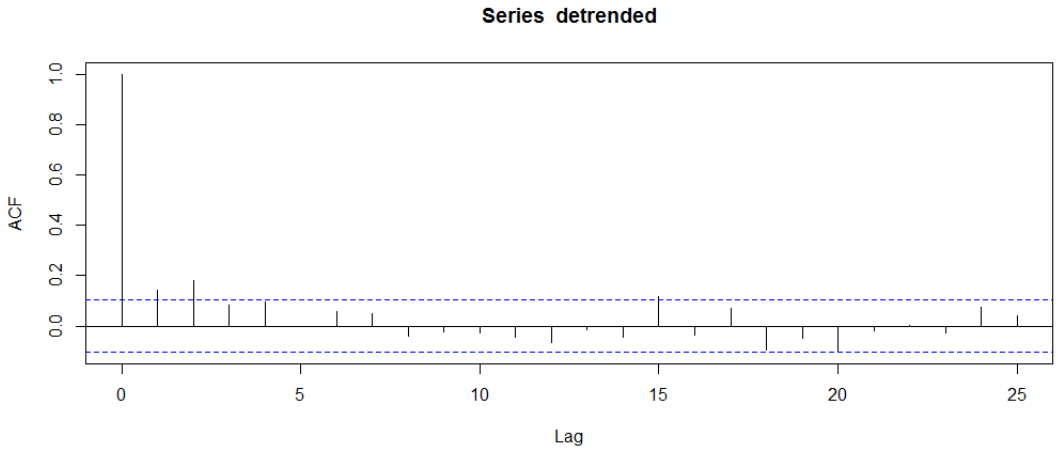

The periodogram in Figure 20 is very cluttered with many peaks. We will look at the two peaks that out (have a periodogram value of higher than 2): at index 4 and index 15, or $\omega_1 = 4/358 = 0.0111$ and $\omega_2 = 15/358 = 0.0419$. We have $I(\omega_1) = 2.811343$ and $I(\omega_2) = 3.007577$ respectively. This yields periods of 89.5 years and 24 years respectively. The 95% confidence intervals are $f(\omega_1) \in [0.407, 59.396]$ and $f(\omega_2) \in [0.381, 55.521]$. However, these are very problematic because the lower

Figure 20:

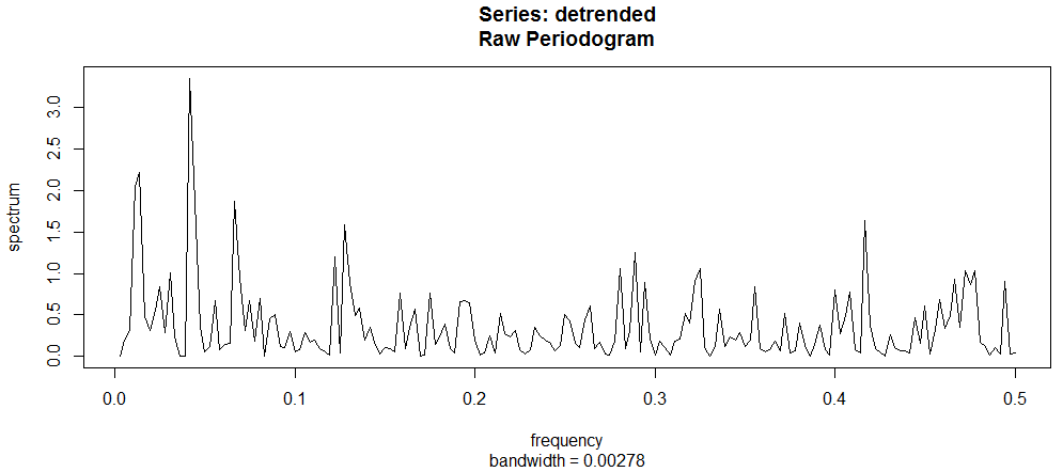

bounds of the confidence intervals are not high enough to make any conclusions regarding the significance of these frequencies. In order to improve such estimates, we will smooth the periodogram. We know from the book that kernel smoothing the periodogram can constrict some of the confidence intervals (allowing us to more accurately assess dominant frequencies) at the expense of flattening out some of the peaks. We present the smoothed periodogram of the yearly averaged temperature data in Figure 21, using the Daniel kernel with parameter $m = 6$. This parameter was chosen experientially, as any lower value gives a periodogram that is far too clustered, and any higher level concentrated lower frequencies too much.

Figure 21:

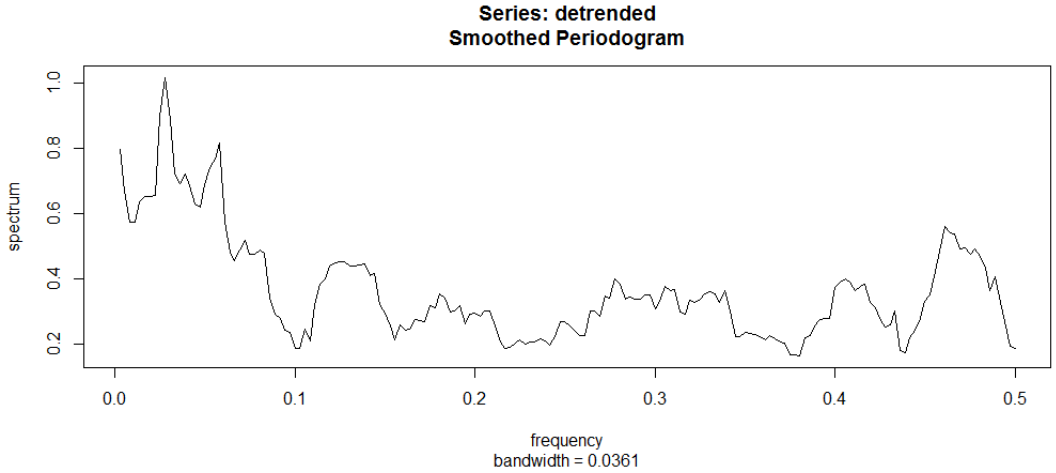

Figure 21 is certainly useful, because it highlights the two frequencies that we previously identified, and smooths away many of the smaller peaks that were disrupting our vision of the data. However, we do not strengthen our conclusion, as those particular frequencies do not rise above their surrounding frequencies enough to be considered indicators of significant regular periodic behavior (the lower bound of their confidence intervals are not high enough). This could reflect the weakness of the non-parmetric techniques for estimating spectral densities. Thus, we will proceed to analyze the spectral distributions from a parametric standpoint. First, however, we will recall that in *section 2* we identified different periodic trends in each of the seasons. As such, we will repeat this analysis on each of the seasons. Figure 22 displays the seasonal data with cubic trends, Figure 23 displays the seasonal de-trended data, Figure 24 contains the periodograms, and Figure 25 displays the smoothed periodograms with $m = 6$. For the sake of brevity, we omit the coefficients of the cubic fits, but rest be assured the coefficients were significant for all polynomials. **Note:** Neither a cubic model nor a quadratic model had significant coefficients for the winter season; this is consistent with our intuition of the data from our visualization in *section 2*. As such, a linear model was fitted instead.

Figure 22: Seasonal Trends

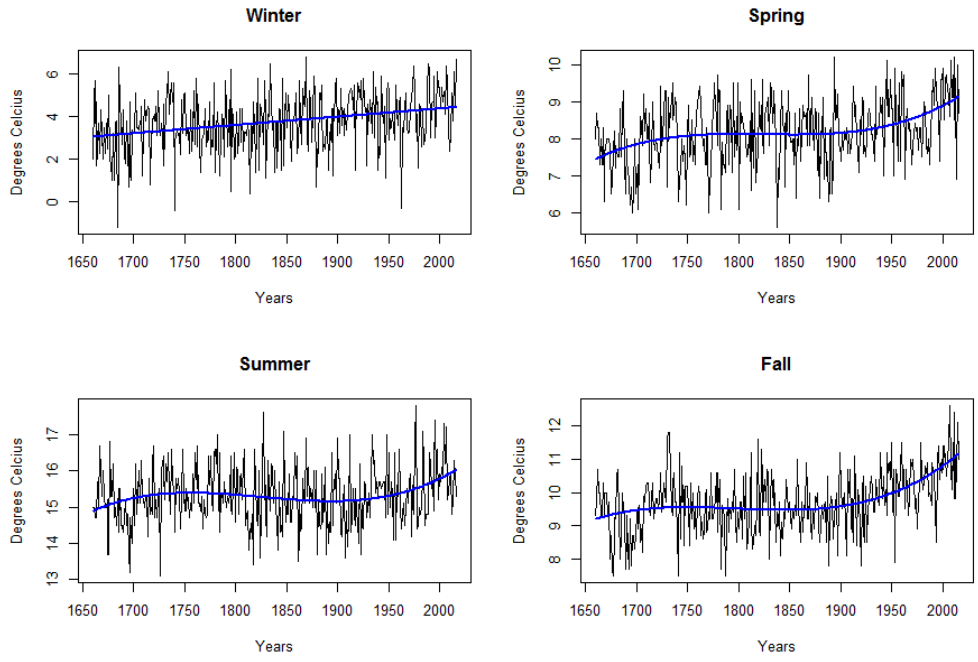

We obtain a lot of new information from the season-by-season analysis, but unfor-

Figure 23: Detrended Seasons

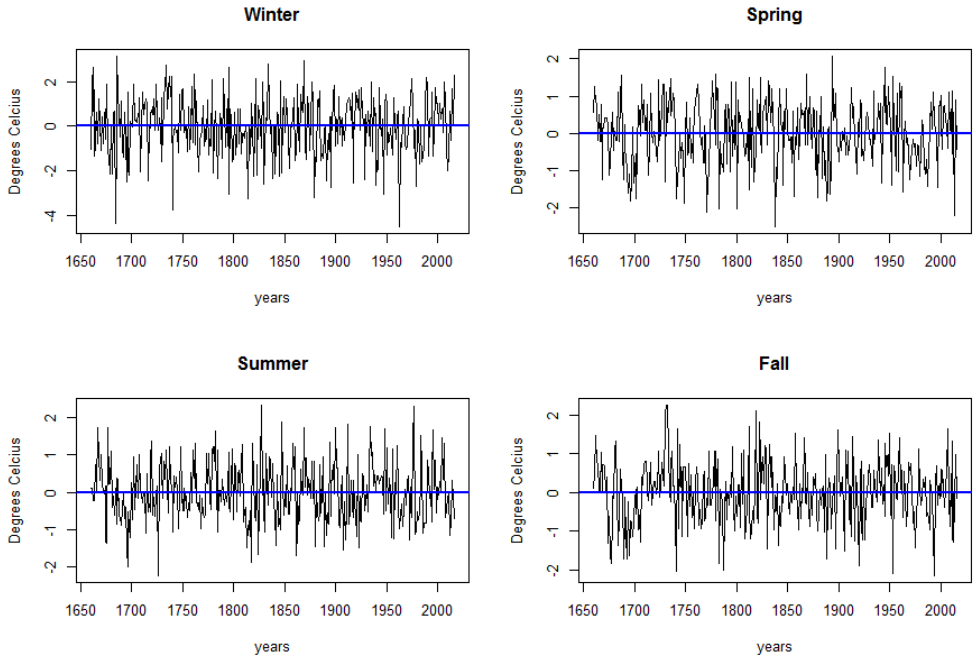

Figure 24: Seasonal Periodograms (Detrended)

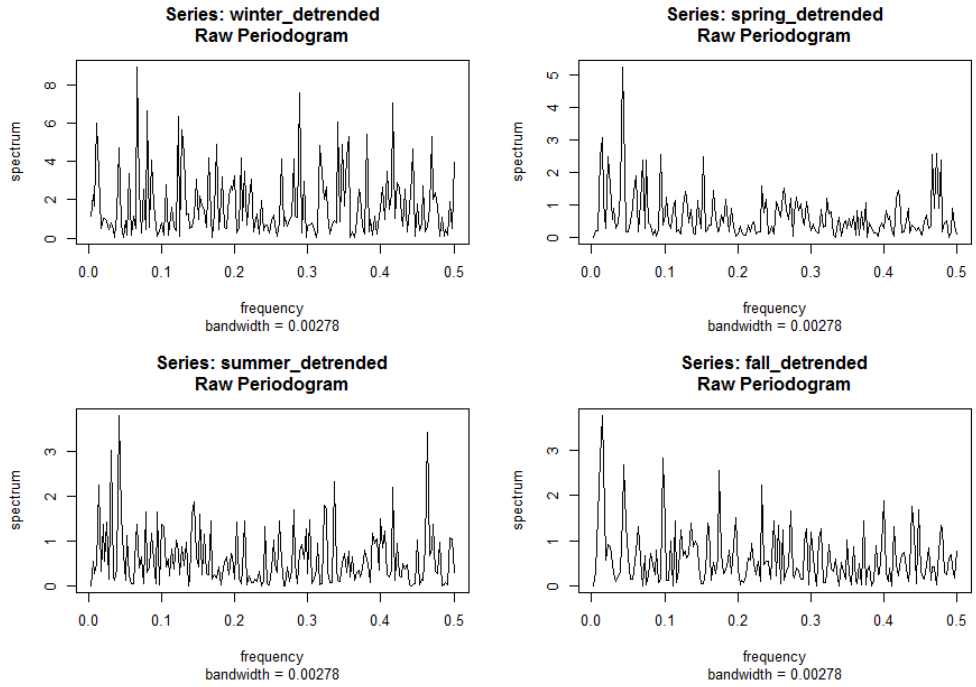

Figure 25: Smoothed Seasonal Periodograms (Detrended)

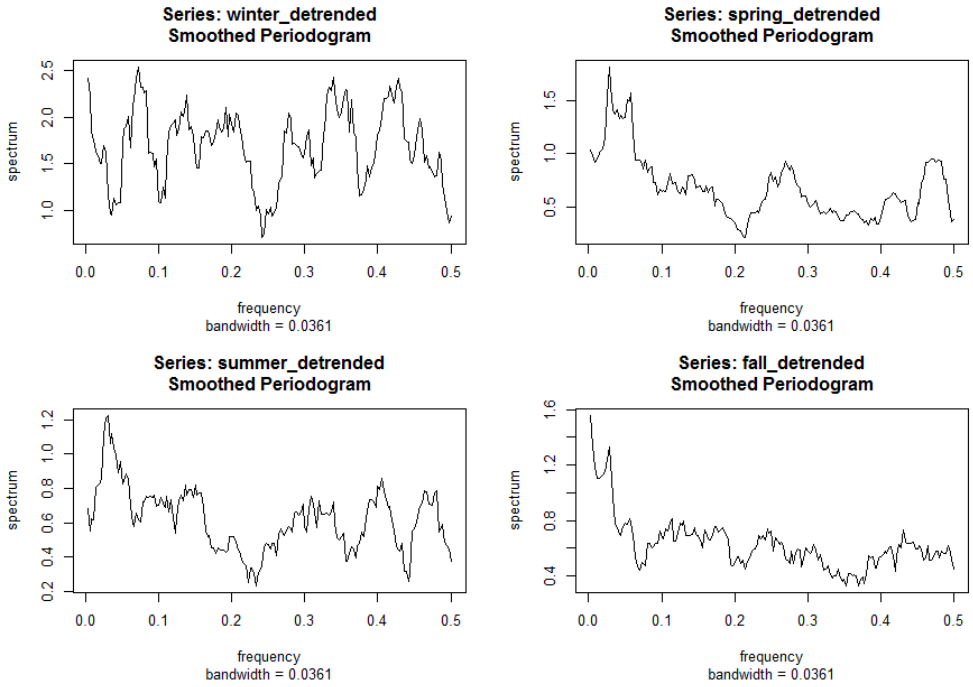

tunately none of it is very significant. We primarily see the difference between the winter season trend and the trends for spring, summer, and fall. From Figure 22, we can see that the cubic trends for the spring, summer, and fall seasons all look fairly similar. However, we are forced to fit a linear trend model to the winter season. As such, the de-trended series in Figure 23 look fairly stationary for spring, summer, and fall, but not as much for winter (we see what appears to be deviations from a mean of zero). This may suggest that we should instead separate our analysis of the time series by season. However, such a strategy would not yield any additional insights as to the periodic behavior of the de-trended series; we say this because the periodograms of Figure 24 are similar to the overall periodogram for spring, summer, and fall, and similar but with more prominent higher-frequency peaks in winter. Smoothing the periodograms in Figure 25 shows similar patterns as well for spring, summer, and fall, with more prominent higher-frequency peaks in winter. Nevertheless none of these peaks are significant in relationship to surrounding frequencies, so we gain little insight about the periodic behavior of the series on the whole.

This lack of insight could be due to the non-parametric nature of this evaluation. Because we are making no assumptions about the data, the significance of any particular peak is less than if we assumed an AR model. As such, we will try using parametric

spectral estimation, specifically auto-regressive spectral estimation, in order to see if there are any significant frequencies. These results should be taken lightly because we have no particular reason to assume an AR structure to the data (in fact, we fit an MA model in the previous section). Figure 26 is the result of running spec.ar on the de-trended yearly averaged series, while Figure 27 is the result of running spec.ar on the de-trended seasonal series respectively.

Figure 26: Auto-regressive Spectral Estimation Yearly Data

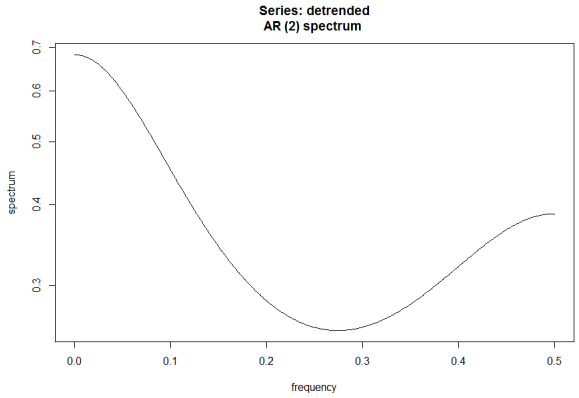

Figure 27: Auto-regressive Spectral Estimation Seasonal Data

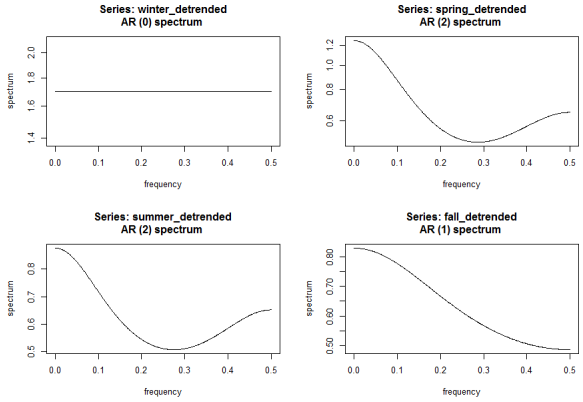

As we can see, no additional insight is gained. Finally, in Figure 28 we plot the coherency between the de-trended series. They are surprisingly non-coherent, with the only significant taking place in in adjacent seasons.

Figure 28: Pairwise Coherency Plots of the Seasons

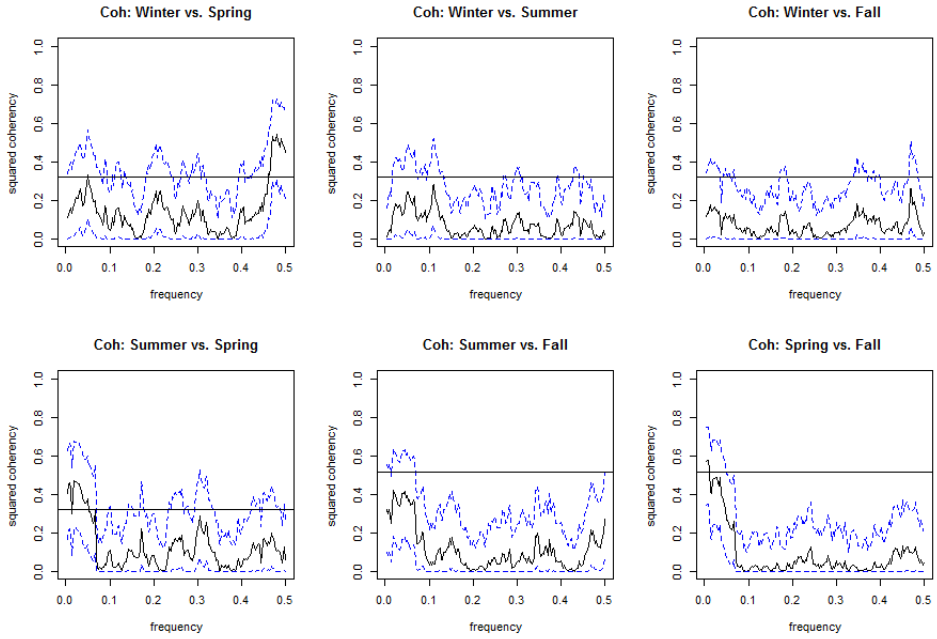

5 Evaluating the Warming Trend

In this section, we will evaluate three claims relating to global warming. The first is the standard man-made global warming hypothesis, specifically that the increase in global temperatures after 1950 are higher than what would be expected given the natural temperature trend (insinuating that the unexplained temperature increases are man-made). We then test the hypothesis that global warming slowed down after 2000 (inspired by Vaidyanathan's article). Finally, we test a stronger man-made global warming hypothesis, specifically that the increase in temperatures after 1900 are higher than would be expected given natural temperature trends. However, all of these conclusions should be taken with a grain of salt, as they rely on our assumption that temperature trend can be fitted by the combination of a third degree polynomial (as done in *section 4*) and an MA(2) model (as done in *section 3*). This assumption is not justified by actual science of global temperature trends, and rather is justified with respect to our observation of the time series (see *section 2*).

Hypothesis One: Warming after 1950 cannot be explained by pre-existing trends

To evaluate this claim, we are going model the pre-1950 temperature series in isolation

from the rest of the data in order to create a predictive model. We will then use that model to create confidence levels of our prediction for the following fifty six years. We then evaluate the hypothesis by comparing the actual observed values (with fitted mean) against our confidence interval. First we will 'de-trend' the data as done in *section 4*, however since we are dealing with a restricted data-set we cannot re-use the fit previously obtained. We determine through running fits of various degrees in R-code that both the linear model and the quadratic model have significant coefficients, so as such we fit a third and fourth degree polynomials as below:

```
Coefficients:
Estimate Std. Error t value Pr(>|t|)
(Intercept) -1.377e+03  4.635e+02  -2.971  0.00322 **
y            2.310e+00  7.722e-01   2.992  0.00301 **
I(y^2)      -1.283e-03  4.284e-04  -2.995  0.00298 **
I(y^3)       2.373e-07  7.912e-08   3.000  0.00294 **
```

```
Coefficients:
Estimate Std. Error t value Pr(>|t|)
(Intercept)  1.477e+04  1.141e+04   1.295    0.196
y           -3.359e+01  2.535e+01  -1.325    0.186
I(y^2)       2.861e-02  2.110e-02   1.356    0.176
I(y^3)      -1.082e-05  7.803e-06  -1.386    0.167
I(y^4)       1.532e-09  1.081e-09   1.417    0.158
```

Since the coefficients of the quartic polynomial are not significant, we conclude that a cubic polynomial is a suitable description of the trend in this restricted dataset. In Figure 29 and Figure 30, we plot the data with trend and the de-trended data respectively. Note that in these graphs, we refer to the time series yearly averaged data from 1659 to 1950 as the 'training data' because we are using this data to 'train' our predictive model.

What we like about this detrended series is that it appears stationary, as the mean seems to be constant around zero the variance appears to be constant with respect to time. However we cannot be sure if the residuals are white noise (which would mean that the model is sufficient) as, in Figure 31, some of the autocorrelations are significant. Running the Box-Ljun test for lag 1, we get:

Figure 29:

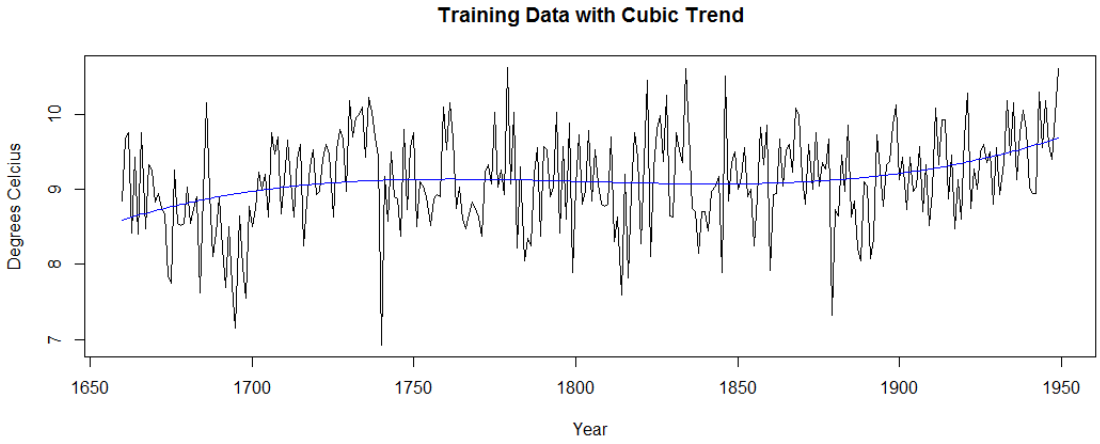

Figure 30:

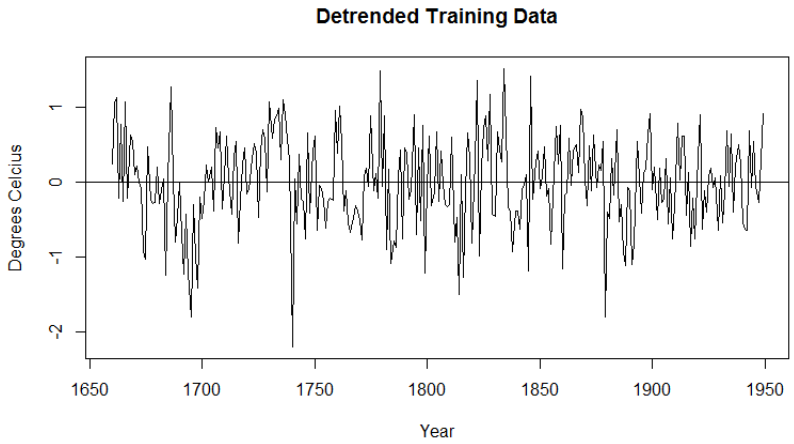


```
Box-Ljung test

data:  detrended
X-squared = 4.1559, df = 1, p-value = 0.04149
```

At the $\alpha = 0.05$ level, we reject the null hypothesis that the series is white noise. As such, we will fit an ARMA model to remove the excess correlation. Because the Aacf seems to taper off and the acf seems to terminate at lag 2, we will fit an MA(2) model, getting the following output (with diagnostic plots in Figure 32):

Figure 31:

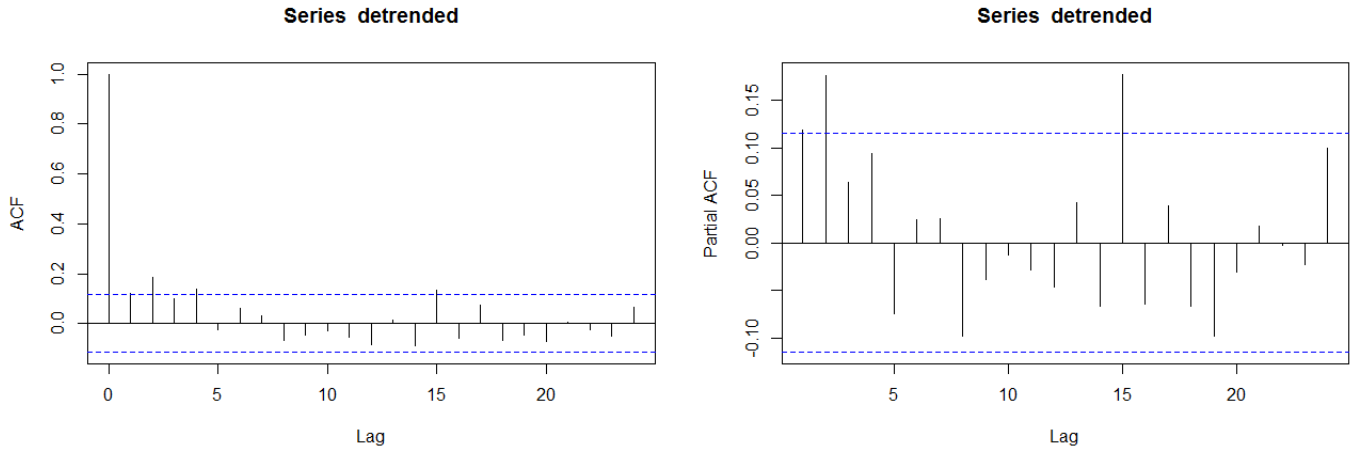


```
Coefficients:
ma1      ma2      xmean
0.0942   0.1596    0.0028
s.e.  0.0586   0.0588   0.0499
```

Figure 32:

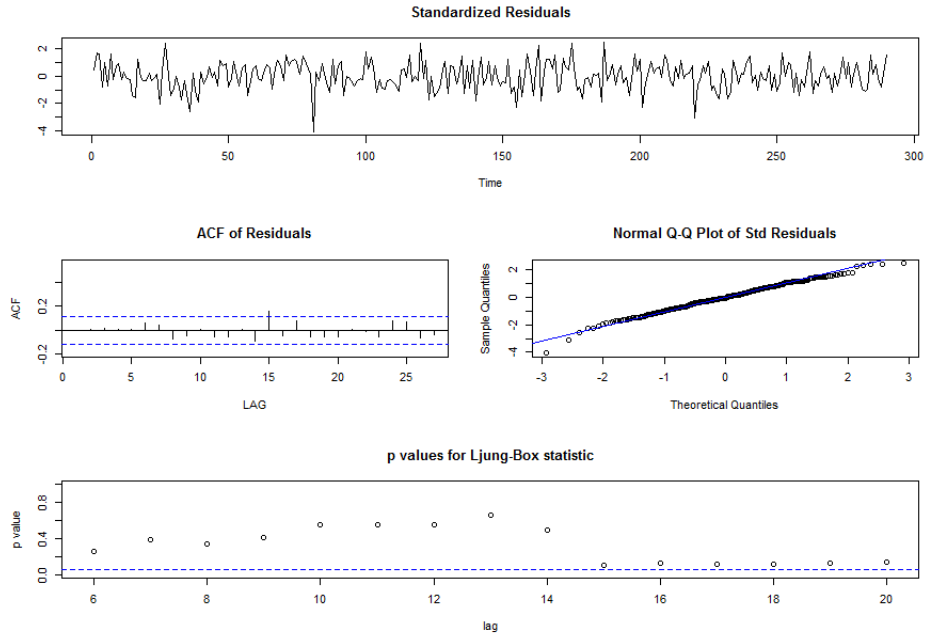

In regards to Figure 32, all of the Ljung-Box p-values are greater than $\alpha = 0.05$, and the Q-Q, acf, and standardized residual plots all check out, we will use this model to predict the temperatures of the years 1950 through 2016. Doing so, we get the following graph, where the green line is the fitted polynomial to the *overall* series (indicating the mean), the red line is the forecasts given the MA(5) model, the blue dotted lines are our 80% confidence interval for the MA(5) predictions, and the purple line is the actual values.

Figure 33:

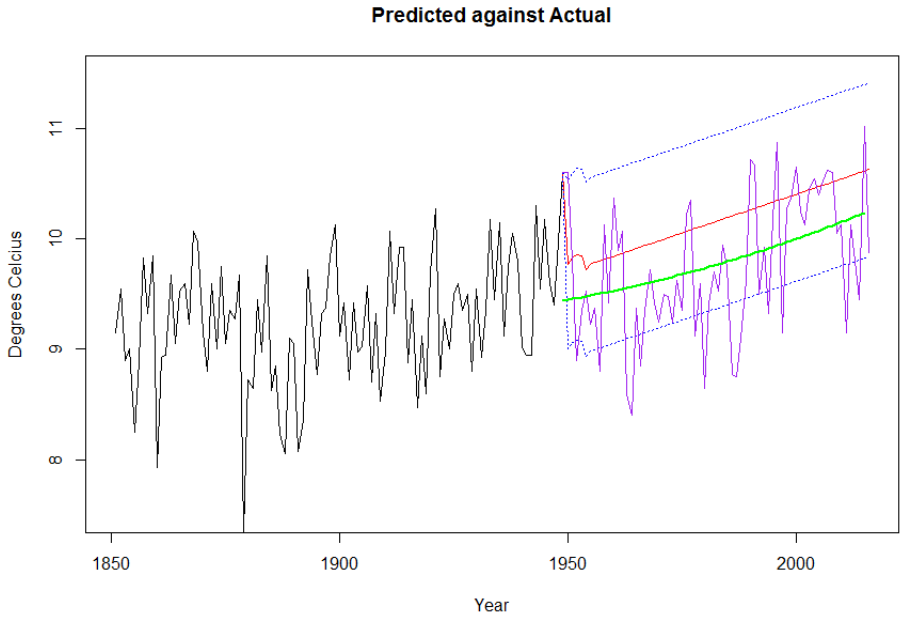

The actual temperatures are almost always in our 80% confidence interval (the projected mean is as well within our confidence interval), so we cannot say that the warming trend after 1950 are unexplained by the general trend. Keep in mind, however, that this insuinates little about *global* because we are only analyzing the data of one location. *Note: Even though we only plot the post-1800 graph, we analyze the entire pre-1950 dataset when assessing trend in this test.*

Training Data 2000 and 1900

In the following plots, we repeat the analysis of the above on two sets of training data, specifically the temperature data before 1900 and the temperature data before 2000. Note that we examine the trend fit, diagnostic plots, acf plots, and et cetera, but omit the plots for the sake of brevity. **Note:** In statistics, it is incorrect to set hypotheses after viewing the data. As such, we do not interpret these different

training sets as indicative of post-viewing data splicing, but rather as testing two hypotheses; our hypothesis for the pre-1900 data is whether or not post-1900 global warming be attributed to natural trends or not man, and our hypothesis for the pre-2000 data is whether or not global warming *slowed down* after 2000. Both of these hypotheses are formulated external to knowledge of the data or its trends. We now present our information graphically: Figure 34 is the plot for the post-1900 training set (with colors consistent with that in the previous prediction graph) while Figure 35 is that for the post-2000 training set.

Figure 34:

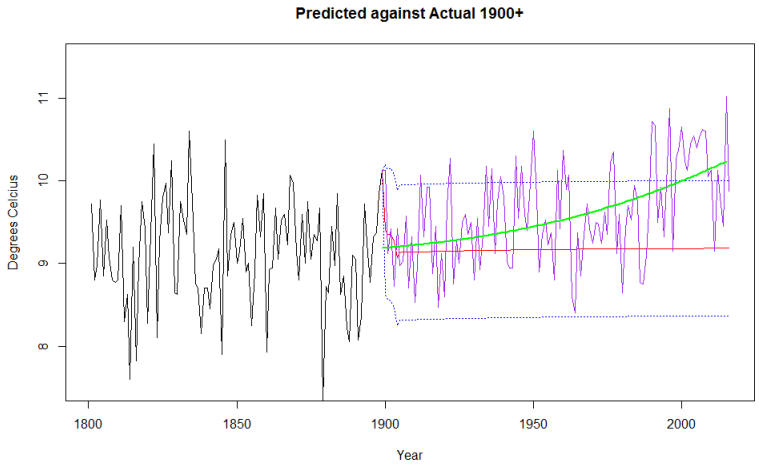

Figure 35:

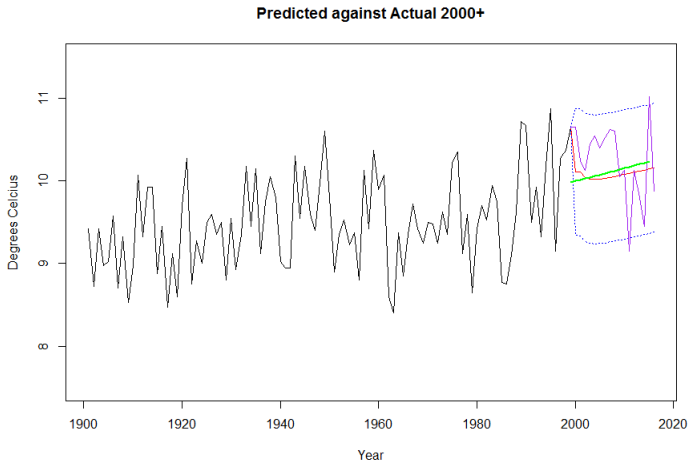

From Figure 34, we conclude that post-1900 warming trends *cannot* be completely

explained by pre-existing temperature trends (in other words, we reject the null hypothesis that the pre-1900 trend explains the post-1900 trend) because the post-1900 trend (indicated by the green line) exits our 80 percent confidence interval. This provides evidence for man-made global warming, despite the fact that the hypothesis does not hold for the pre-1950 data (which hypothesis is used depends on when one considers the beginning of 'man-made' influence). On the other hand, for the post-2000 data set the predicted mean (in red) and the post-2000 mean (in green) are very close, indicating that pre-2000 trends fairly accurately describe the post-2000 trend. This indicates evidence against the hypothesis that warming 'slowed down' after 2000 as suggested in the article.

6 Conclusion

In this project, we analyze the central England temperature dataset with a variety of methods, and then test three general hypotheses regarding warming trends. Our main conclusion is that we reject the null hypothesis that modern warming trends are explained by pre-existing trends at the 1900 cutoff, but not at the 1950 cutoff. Rejecting the null hypothesis provides evidence for man-made global warming, however we cannot generalize too much because we only examine one location of temperature data, and from our perspective there is nothing to say that the unexplained rise in temperatures is not due to some other factor other than man made influence. As previously mentioned, the papers of Jones and Bradley (1992a), Benner (1999) and Vaidyanathan (2016) also discuss this dataset. Our results agree with the temperature warming conclusion of Jones and Bradley, who claim on page 263 that significant warming has occurred since 1850 (while our results claim that it is significant after 1900; we did not consider a pre-1900 dataset but presumably would have achieved analogous results). Our results do not corroborate the results of Benner, who identified periodic components in the temperature data that he attributed to sunspots and the North Atlantic Oscillation, because none of the models that we fit had any significant periodogram frequencies (Benner claims that "Fourier spectra have poor frequency resolution at lower frequencies"(Benner 393), and as such uses other methods such as wavelet analysis and the the Lomb–Scargle periodogram to analyze periodicity). Finally, our results provide evidence against the idea in Vaidyanathan that global temperature increases slowed down in the last decade, as our pre-2000 model predicts temperatures of the last decade with a 80% confidence interval and none of the year-averaged temperature values were significant. This does not given any evidence of a 'slow down' in the increasing temperature trend, at least at this particular location.